Macromolecular crowding compacts unfolded apoflavodoxin and causes severe aggregation of the off-pathway intermediate during apoflavodoxin unfolding.

Engel, R.; Westphal, A.H.; Huberts, D.H.E.W.; Nabuurs, S.M.; Lindhoud, S.; Visser, A.J.W.G.; Van Mierlo, C.P.M.

published in
Journal of Biological Chemistry
2008

DOI (link to publisher)
10.1074/jbc.M802393200

document version
Publisher's PDF, also known as Version of record

THE JOURNAL OF BIOLOGICAL CHEMISTRY VOL. 283, NO. 41, pp. 27383–27394, October 10, 2008

Macromolecular Crowding Compacts Unfolded Apoflavodoxin and Causes Severe Aggregation of the Off-pathway Intermediate during Apoflavodoxin Folding*

Received for publication, March 27, 2008, and in revised form, June 13, 2008 Published, JBC Papers in Press, July 18, 2008, DOI 10.1074/jbc.M802393200

Ruchira Engel[‡1], Adrie H. Westphal[‡], Daphne H. E. W. Huberts[‡], Sanne M. Nabuurs[‡], Simon Lindhoud[‡], Antonie J. W. G. Visser[§], and Carlo P. M. van Mierlo[‡2]

From the [‡]Laboratory of Biochemistry, MicroSpectroscopy Centre, Wageningen University, Dreijenlaan 3, 6703 HA, Wageningen, The Netherlands and the [§]Department of Structural Biology, Institute of Molecular Cell Biology, Vrije Universiteit, De Boelelaan 1085, 1081 HV Amsterdam, The Netherlands

To understand how proteins fold *in vivo*, it is important to investigate the effects of macromolecular crowding on protein folding. Here, the influence of crowding on *in vitro* apoflavodoxin folding, which involves a relatively stable off-pathway intermediate with molten globule characteristics, is reported. To mimic crowded conditions in cells, dextran 20 at 30% (w/v) is used, and its effects are measured by a diverse combination of optical spectroscopic techniques. Fluorescence correlation spectroscopy shows that unfolded apoflavodoxin has a hydrodynamic radius of 37 ± 3 Å at 3 M guanidine hydrochloride. Förster resonance energy transfer measurements reveal that subsequent addition of dextran 20 leads to a decrease in protein volume of about 29%, which corresponds to an increase in protein stability of maximally 1.1 kcal mol^{-1}. The compaction observed is accompanied by increased secondary structure, as far-UV CD spectroscopy shows. Due to the addition of crowding agent, the midpoint of thermal unfolding of native apoflavodoxin rises by 2.9 °C. Although the stabilization observed is rather limited, concomitant compaction of unfolded apoflavodoxin restricts the conformational space sampled by the unfolded state, and this could affect kinetic folding of apoflavodoxin. Most importantly, crowding causes severe aggregation of the off-pathway folding intermediate during apoflavodoxin folding *in vitro*. However, apoflavodoxin can be over expressed in the cytoplasm of *Escherichia coli*, where it efficiently folds to its functional native form at high yield without noticeable problems. Apparently, in the cell, apoflavodoxin requires the help of chaperones like Trigger Factor and the DnaK system for efficient folding.

The spontaneous folding of an unfolded and thus expanded protein to its compact and functional native state is dictated by its amino acid sequence (1). Numerous studies on the refolding of chemically and thermally denatured proteins have brought us closer to understanding how the complex process of protein folding works. However, these *in vitro* folding studies are generally performed in simple buffer systems with low concentrations of protein, whereas the environment in which a protein folds *in vivo* is very different. The cell interior is densely crowded with soluble and nonsoluble macromolecules, which are present in high concentrations (2, 3). In *Escherichia coli* cells, the total concentration of protein and RNA is in the range of 300–400 g/liter (4). These macromolecules collectively occupy 10–40% of the total fluid volume, restricting the volume available to any given macromolecule. In crowded solutions, all processes that result in reduction of the total volume occupied by any given macromolecular species are favored, and this is expected to affect all macromolecular reactions and equilibria, including protein folding (2, 5–8).

Crowding is predicted to affect protein folding in several manners (9, 10). First, crowding destabilizes expanded unfolded protein conformations. As a result, these expanded protein molecules collapse to more compact conformations, and consequently protein folding is enhanced. Compaction of unfolded conformations due to the presence of inert macromolecular crowding agents has been demonstrated for reduced and carboxyamidated RNase T1, cytochrome *c*, and RNase A (11–13). Destabilization of the unfolded state due to the presence of crowding agents should increase the stability of proteins against thermal and chemical denaturation, and this stabilizing effect has indeed been reported for proteins like lysozyme, FK506-binding protein, and apomyoglobin (12, 14–16). Second, macromolecular crowding enhances undesirable aggregation of partially unfolded proteins (17, 18). Irreversible unfolding due to aggregation of unfolded states in the presence of crowding agents has been observed for reduced lysozyme, rabbit muscle creatine kinase, dihydrofolate reductase, enolase, and green fluorescent protein (19–21).

Here, we report several aspects of how crowding affects the folding of a 179-residue flavodoxin from *Azotobacter vinelandii*. Flavodoxins are electron carriers and consist of a single structural domain that adopts the α-β parallel topology, also known as the flavodoxin-like fold, which is widely prevalent in nature (22–24). Understanding the folding of flavodoxin contributes to clarification of the folding behavior of the many proteins that share the flavodoxin-like topology. Both the denatur-

* This work was supported by the Netherlands Organization for Scientific Research "From Molecule to Cell" program. The costs of publication of this article were defrayed in part by the payment of page charges. This article must therefore be hereby marked "*advertisement*" in accordance with 18 U.S.C. Section 1734 solely to indicate this fact.

[1] Present address: Faculty of Biological Sciences, University of Leeds, Leeds LS2 9JT, United Kingdom.

[2] To whom correspondence should be addressed: Laboratory of Biochemistry, Wageningen University, Dreijenlaan 3, 6703 HA Wageningen, The Netherlands. Tel.: 31-317-484621; Fax: 31-317-484801; E-mail: carlo.vanmierlo@wur.nl.

ant-induced equilibrium and kinetic (un)folding of flavodoxin and apoflavodoxin (*i.e.* flavodoxin without the noncovalently bound FMN cofactor) have been characterized in detail using GuHCl[3] as denaturant (24–30). The folding data show that apoflavodoxin autonomously folds to its native state and that FMN does not act as a nucleation site for folding. NMR spectroscopy shows that apoflavodoxin is structurally identical to flavodoxin except for considerable dynamics of residues in the flavin-binding region (31, 32). In the presence of FMN, binding of the FMN cofactor to native apoflavodoxin is the last step in flavodoxin folding.

The GuHCl-induced equilibrium (un)folding of apoflavodoxin is described by the three-state mechanism N ⇔ U ⇔ I_{off}, in which N is the native state, U is the unfolded state, and I_{off} is an off-pathway folding intermediate (27). The off-pathway intermediate has molten globule-like properties and populates to significant extents at denaturant concentrations ranging from about 1 to 3 M GuHCl. This folding species has ~65% of the α-helical content observed for native apoflavodoxin but lacks the characteristic tertiary structure of the native state. Also in this state, the three tryptophans of apoflavodoxin are exposed to solvent as opposed to the situation in native protein (25, 27). Part of the conformation of the intermediate is ordered and exchanges between different conformers on the micro- to millisecond time scale, and another part of the folding species is unfolded.[4] This relatively compact intermediate acts as a trap during kinetic folding of apoflavodoxin. The formation of such an off-pathway species, which needs to unfold to allow folding to proceed to the native state, is typical for the topology of apoflavodoxin (29). Despite the considerable population of the folding intermediate, which is inferred to be highly aggregation-prone due to exposed hydrophobic groups, denaturant-induced apoflavodoxin unfolding is fully reversible up to a 6 μM protein concentration. An off-pathway intermediate is also likely to populate during thermally induced unfolding of apoflavodoxin (25).

Currently, the impact of macromolecular crowding on the autonomous folding of *A. vinelandii* apoflavodoxin *in vitro* is unknown and is therefore addressed in this study. To investigate the effect of crowding on GuHCl-induced apoflavodoxin (un)folding, we made use of 30% (w/v) dextran 20, since this condition mimics the crowded circumstances in the cytoplasm of cells (4) and because the use of dextrans as macromolecular crowding agents is well described (12, 17, 33, 34). Dextrans are uncharged, inert polysaccharides. The effects of added dextran on a variety of reactions have been attributed to excluded volume (34–40). The effects of dextrans on the properties of the different apoflavodoxin folding species are investigated using intrinsic tryptophan fluorescence and CD spectroscopy. Thermal denaturation of apoflavodoxin in the absence and in the presence of crowding agent was followed with fluorescence emission spectroscopy. The hydrodynamic radii of apoflavodoxin folding species are determined with fluorescence correlation spectroscopy (FCS). In addition, single-pair Förster resonance energy transfer (FRET) is measured to study whether crowding leads to compaction of unfolded apoflavodoxin molecules using protein molecules that are covalently labeled with donor and acceptor fluorophores.

EXPERIMENTAL PROCEDURES

Sample Preparation—Recombinant *A. vinelandii* wild-type and C69A flavodoxin were expressed in *E. coli* cells and purified as described previously (25). Apoflavodoxin was subsequently prepared by trichloroacetic acid precipitation (25) and purified by gel filtration on a Superdex 75 HR column (Amersham Biosciences) to remove oligomeric species. The protein concentration was determined spectrophotometrically using an extinction coefficient of 29 mM^{-1} cm^{-1} at 280 nm. Purified apoflavodoxin was aliquoted and stored at −20 °C. In all experiments except for the ones utilizing dye-labeled protein molecules, the C69A variant of apoflavodoxin was used, in which the single cysteine residue 69 is replaced by an alanine residue to avoid covalent dimerization of apoflavodoxin. This protein variant is similar to wild-type apoflavodoxin regarding both redox potential of holoprotein and stability of apoprotein (25, 41).

Wild-type apoflavodoxin was labeled with AlexaFluor 488 (A488) maleimide (Invitrogen) at cysteine 69. Freshly prepared apoflavodoxin was incubated overnight in the dark at 4 °C with the dye, at a molar ratio of 1:15, in 100 mM potassium pyrophosphate buffer, pH 8. The free label and protein were separated using an Econo-Pac 10DG column (Bio-Rad) followed by gel filtration on a Superdex 75 HR column. The purified labeled protein in potassium pyrophosphate buffer (100 mM, pH 6.0) was subsequently aliquoted and stored at −80 °C. Preparation of the S178C variant of wild-type flavodoxin and subsequent site-specific labeling of Cys-69 with A488 and of Cys-178 with AlexaFluor 568 (A568) (Invitrogen) will be described elsewhere.

GuHCl (Sigma) and dextrans with average molecular masses of 6 kDa (dextran 06), 20 kDa (dextran 20), and 70 kDa (dextran 70) (Fluka Biochemika, The Netherlands) were used without further purification. All stocks and samples were prepared in 100 mM potassium pyrophosphate (Sigma) buffer, at pH 6. Samples containing dextran were prepared by adding the required quantity of dextran stock, which ranged from 40 to 60% (w/v), to apoflavodoxin in buffer at different concentrations of GuHCl.

Fluorescence Correlation Spectroscopy—FCS measurements were performed on a ConfoCor 2 setup (Carl Zeiss, Germany). The details of the setup have been described before (42). Samples were excited with the 488-nm laser line from an argon-ion laser, which was focused with a water-immersion C-apochromat ×40 objective lens (Carl Zeiss). Fluorescence was detected by an avalanche photodiode after being filtered through a 505–550-nm band pass filter. Excitation power was ~11 microwatts.

Measurements were performed on samples contained in a glass bottom microplate with 8 wells (Nunc chambered coverglass; Lab-tech, Wiesbaden, Germany), which was maintained at 25 °C with the help of a water bath. Samples were allowed to equilibrate for 5 min before the start of each measurement. Each sample contained 25 nM dye-labeled apoflavodoxin. To

[3] The abbreviations used are: GuHCl, guanidine hydrochloride; A488 and A568, AlexaFluor 488 and 568 dye label, respectively; FCS, fluorescence correlation spectroscopy; FRET, Förster resonance energy transfer.

[4] S. M. Nabuurs, personal communication.

minimize adsorption of dye-labeled protein, ~4 μM nonlabeled protein was added to all samples. Five FCS data traces, each of 60 s duration, were recorded of each sample.

FCS data were analyzed using FCS Data Processor version 1.5 (43). The autocorrelation function $G(\tau)$ was fitted with a model that describes Brownian motion of a single species in three dimensions with an additional term for fast fluctuations due to molecules entering a nonfluorescent triplet state (44).

$$G(\tau) = 1 + \frac{1}{N} \cdot \frac{\left(1 + \frac{F_{trip} e^{-\tau/T_{trip}}}{1 - F_{trip}}\right)}{\left(1 + \frac{\tau}{\tau_d}\right)\sqrt{1 + \left(\frac{\omega_{xy}}{\omega_z}\right)^2 \frac{\tau}{\tau_d}}} \quad \text{(Eq. 1)}$$

Here, N represents the average number of molecules present in the confocal detection volume, τ_d is the diffusion time, ω_{xy} and ω_z are the equatorial and axial radii of the confocal volume, respectively, F_{trip} is the fraction of molecules in the nonfluorescent triplet state, and T_{trip} is the relaxation time of the triplet state. During analysis, τ_d values obtained from repeat FCS measurements using the same sample were linked. The ratio ω_z/ω_{xy} was determined by calibration with a solution containing free A488 molecules and varied between 5 and 8 for different samples. The diffusion time τ_d is related to the diffusion coefficient (D) according to Equation 2,

$$\tau_d = \frac{\omega_{xy}^2}{4D} \quad \text{(Eq. 2)}$$

in which ω_{xy} of the instrumental setup was calculated using rhodamine 110. For samples in buffer, ω_{xy} was ~150 nm.

The Stokes-Einstein equation relates the diffusion time of a globular species to its hydrodynamic radius (r_h),

$$D = \frac{kT}{6\pi \cdot n \cdot r_h} \quad \text{(Eq. 3)}$$

in which k is the Boltzmann constant, T is the temperature in Kelvin, and n is the viscosity of the solution. Taking τ_d obtained for native apoflavodoxin at 25 °C in buffer ($n = 1 \times 10^{-3}$ centipoises) and using Equations 2 and 3, the corresponding hydrodynamic radius of the native molecule was calculated.

The hydrodynamic radius of apoflavodoxin at different GuHCl concentrations was calculated from the corresponding diffusion times of dye-labeled apoflavodoxin measured with FCS. Upon increasing the concentration GuHCl, solvent viscosity and refractive index also increase, and thus the dimensions of the confocal volume are affected, giving rise to an apparently larger τ_d (45). To correct for these changes, the ratio of τ_d of the dye-labeled protein at a specific GuHCl concentration and the τ_d of free A488 at exactly the same GuHCl concentration ($\tau_{d\,apo,[GuHCl]}/\tau_{d\,A488,[GuHCl]}$) was calculated. Assuming that the hydrodynamic radius of A488 is unaffected by GuHCl, the change in τ_d of A488 is entirely due to viscosity and refractive index influences caused by GuHCl. Thus, the changes in apoflavodoxin-A488 diffusion relative to the diffusion of free A488 molecules are independent of refractive index and viscosity effects and are proportional to the real change in protein hydrodynamic radius as it unfolds. The average hydrodynamic radius of apoflavodoxin at a given GuHCl concentration ($r_{apo,[GuHCl]}$) is calculated according to Equation 4,

$$r_{apo,[GuHCl]} = r_{apo,0M} \cdot \left(\frac{\tau_{d\,apo,[GuHCl]}}{\tau_{d\,A488,[GuHCl]}}\right)\left(\frac{\tau_{d\,A488,0M}}{\tau_{d\,apo,0M}}\right) \quad \text{(Eq. 4)}$$

in which $\tau_{d\,apo}$ and $\tau_{d\,A488}$ are the diffusion times of dye-labeled apoflavodoxin and A488, respectively, and the subscript [GuHCl] refers to the concentration of GuHCl used.

Fluorescence Spectroscopy—Steady-state fluorescence measurements were performed using a Cary Eclipse fluorimeter (Varian; Bergen op Zoom, The Netherlands) equipped with a Peltier accessory (Varian) for temperature control.

Emission spectra ranging from 300 to 700 nm of apoflavodoxin in different solvents were obtained by exciting samples at 280 nm. The emission and excitation slits were set at 5 nm. Protein concentration in all samples was 2 μM.

Protein Refolding Followed by Fluorescence Emission—In the case of refolding measurements, fluorescence intensity of the different apoflavodoxin samples before and after dilution of denaturant was acquired for a period of 30 s at 340 nm and subsequently averaged. Before dilution, protein concentration in all samples was 2 μM. Crowding agent was added to 30% (w/v) to apoflavodoxin unfolded in a final concentration of 2 or 3 M GuHCl. After about 30 min, both solutions were diluted 10-fold through the addition of buffer that also contained 30% (w/v) dextran 20. The recovery of native protein in terms of percentage of fluorescence intensity at 340 nm was compared with the fully reversible recovery of native protein in an experiment in which no crowding agent was present. Temperature was maintained at 25 °C.

Determination of Förster Resonance Energy Transfer in Dye-labeled Apoflavodoxin—S178C apoflavodoxin, labeled with A488 at Cys-69 and with A568 at Cys-178, was excited at 475 nm, and subsequently fluorescence emission spectra ranging from 480 to 700 nm were recorded in various solvent conditions at 25 °C. Protein concentration in all samples was 84 nM. The excitation slit was set at 2.5 nm, and the emission slit was set at 5 nm. To avoid loss of signal due to protein adsorption, 0.001% Tween 20 (v/v) was also added to the samples. This addition does not affect apoflavodoxin folding. Similarly, fluorescence emission spectra of wild-type apoflavodoxin labeled with A488 at position Cys-69 (donor only) and present in identical solvent conditions as double dye-labeled S178C apoflavodoxin were obtained under an identical instrumental setup. All fluorescence emission spectra were corrected by subtracting emission spectra of the corresponding blank solutions.

The Förster radius (R_0) of the A488/A568 pair attached to apoflavodoxin was calculated according to Ref. 46,

$$R_0^6 = 8.785 \cdot 10^{23} \cdot \kappa^2 \cdot Q_D \cdot J \cdot \eta^{-4} \quad \text{(Eq. 5)}$$

in which, κ^2 is the orientation factor for the donor and acceptor transition dipole moments, Q_d is the quantum yield of the donor, J is the spectral overlap between donor emission and acceptor absorption (in M^{-1} cm^3), and η is the refractive index of the medium between the two dyes. R_0 was calculated according to Equation 5, taking into account that both donor and acceptor fluorophores are randomly oriented ($\kappa^2 = 2/3$). Time-

resolved fluorescence anisotropy measurements of labeled apoflavodoxin molecules show that the dyes exhibit rapid rotational motions (data not shown). The values of Q_d and J of the fluorophores attached to apoflavodoxin were determined at each solvent condition used. Q_d for protein in buffer is 0.84 ± 0.03, and Q_d for protein in buffer containing 30% (w/v) dextran is 0.74 ± 0.03. Upon the addition of GuHCl, Q_d reduces; for protein in buffer containing 3 M GuHCl, Q_d is 0.57 ± 0.02, and for protein in buffer containing 3 M GuHCl and 30% (w/v) dextran, Q_d is 0.50 ± 0.02. J was calculated to be 3.0 ± 0.1 10^{-13} M^{-1} cm^3 using a value of 91,300 M^{-1} cm^{-1} for the extinction coefficient of A568. We have used a value of 1.60 ± 0.02 for the refractive index for the folded protein (47–49). The solvent refractive indices are 1.389345 ± 0.000003 for 3 M GuHCl and 1.431550 ± 0.000003 for 3 M GuHCl containing 30% (w/v) dextran. Thus, the value of η used for the calculation is 1.50 ± 0.02 for protein in 3 M GuHCl, and η is 1.52 ± 0.02 for 3 M GuHCl containing 30% (w/v) dextran, assuming that the medium between the dyes is composed of 50% protein and 50% solvent (50). Using the values given above and Equation 5, we calculate that R_0 for protein in 3 M GuHCl is 52.0 ± 0.5 Å, and R_0 for denatured protein in 3 M GuHCl containing 30% (w/v) dextran is 50.4 ± 0.5 Å. A similar calculation for the protein in buffer, in the absence and in the presence of dextran, leads to R_0 of 53.1 ± 0.5 and 52.0 ± 0.5 Å, respectively.

FRET efficiencies (E) were calculated using Equation 6,

$$E = 1 - \frac{F_{DA}}{F_D} \qquad \text{(Eq. 6)}$$

where F_{DA} is the intensity of donor in the presence of acceptor, and F_D is the intensity of donor only, both determined at the emission maximum of the donor (*i.e.* at 522 nm, when the donor is attached to Cys-69 of apoflavodoxin) and at equal absorbances at the excitation wavelength. The distance between donor and acceptor (R) was calculated using Equation 7,

$$R = R_0 \sqrt[6]{\frac{1}{E} - 1} \qquad \text{(Eq. 7)}$$

Thermal Unfolding Measurements—Thermal unfolding of apoflavodoxin was achieved by increasing the temperature from 25 to 65 °C at a rate of 0.5 °C/min, unless mentioned otherwise. The protein was excited at 280 nm, and fluorescence emission was recorded at 330, 340, and 350 nm. The excitation and emission slits were set at 5 nm. Protein concentration in all experiments was ~2 μM. The unfolding curves obtained were globally fit to Equation 8,

$$F = \frac{(a_n + b_n T) + (a_u + b_u T)e^{-\Delta G_u(T)/RT}}{1 + e^{-\Delta G_u(T)/RT}} \qquad \text{(Eq. 8)}$$

in which F is the observed fluorescence intensity at a given temperature T, and a and b are the intercept and slope, respectively, of pretransition (subscript n) and post-transition (subscript u) base lines. R is the molar gas constant. $\Delta G_u(T)$ is the change in free energy upon protein unfolding and is defined as follows,

$$\Delta G_u(T) = \begin{bmatrix} \Delta H_m(1 - T/T_m) \\ -\Delta C_p((T_m - T) + T\ln(T/T_m)) \end{bmatrix} \qquad \text{(Eq. 9)}$$

in which ΔH_m and ΔC_p are the changes in enthalpy and heat capacity associated with protein unfolding, respectively. T_m is the midpoint of the thermal unfolding curve, the temperature at which $\Delta G_u(T) = 0$.

Circular Dichroism Spectroscopy—CD spectra were obtained on a Jasco J715 spectropolarimeter (Tokyo, Japan) using quartz cuvettes (Starna, Hainault, UK) with 1-mm cell length. In case of far-UV CD measurements, 10 wavelength scans of 4 μM protein were acquired, and the resulting spectra were subsequently averaged. In case of near-UV measurements, 15 wavelength scans of 23.5 μM protein were acquired, and the resulting spectra were averaged. All scans were obtained at a rate of 20 nm/min. All CD spectra of apoflavodoxin were corrected by subtracting the CD spectra of the corresponding blank solutions. Temperature was maintained at 25 °C.

RESULTS

Hydrodynamic Radii of Apoflavodoxin Folding Species in the Absence of Crowding—The hydrodynamic radius of apoflavodoxin molecules at various stages of GuHCl-induced denaturation was determined using A488-labeled apoflavodoxin and FCS. Labeling with A488 only marginally destabilized native apoflavodoxin (data not shown).

A model that describes diffusion of a single protein species in three dimensions with diffusion time τ_d (Equation 1) fits very well to the FCS data obtained for apoflavodoxin at all concentrations GuHCl used. Consequently, in the range of 1–3 M denaturant, τ_d is an averaged property that reflects the contribution of the various apoflavodoxin states that are populated (Fig. 1*B*). Using the average diffusion time τ_d as input, the hydrodynamic radius of protein molecules can be derived using Equations 2 and 3. However, increasing the concentration of GuHCl led to alterations in viscosity and refractive index of the solution, and as a result, the apparent diffusion time of a protein molecule became larger. Both of these alterations can be accounted for by the use of Equation 4, which leads to the correct average hydrodynamic radius of apoflavodoxin at different concentrations of GuHCl. As expected, upon apoflavodoxin unfolding, its hydrodynamic radius increased (Fig. 1*A*).

In the absence of denaturant, the native state of apoflavodoxin was fully populated, and FCS measurements show that the hydrodynamic radius of the folded protein molecule was 28 ± 1 Å. At 4 M GuHCl, the unfolded state of apoflavodoxin was fully populated, and no native nor intermediate folding species were present (Fig. 1*B*) (27). FCS demonstrates that at this denaturant concentration, the hydrodynamic radius of unfolded apoflavodoxin is 38 ± 4 Å, a 36% increase compared with the corresponding radius of native protein (*i.e.* 150% increase in volume). Dynamic light scattering experiments with nonlabeled apoflavodoxin confirmed both hydrodynamic radii reported here (data not shown). The hydrodynamic radius of the off-pathway folding intermediate cannot be determined directly from FCS data, because this species is not fully populated at any concentration of GuHCl. However, the hydrodynamic radius of this species can be inferred by taking into

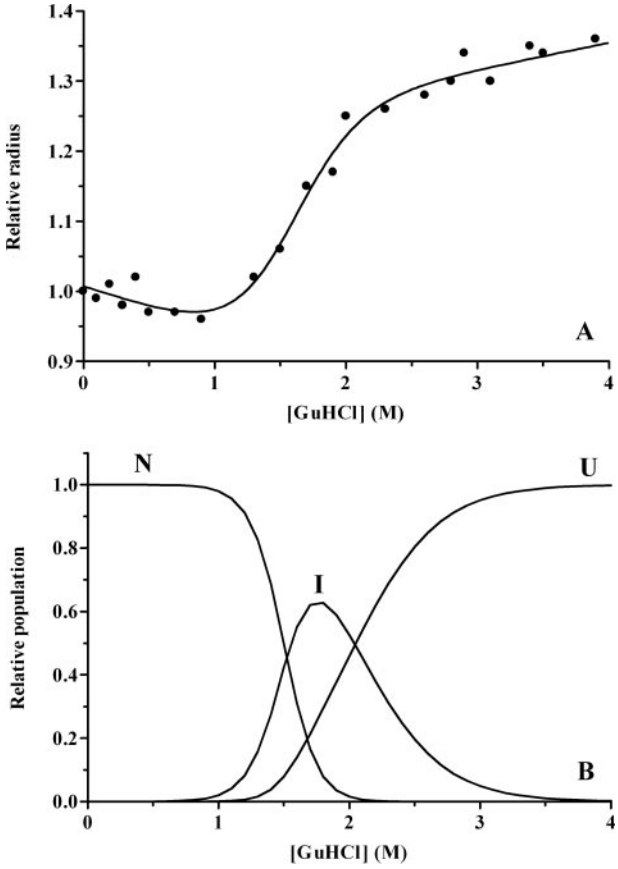

FIGURE 1. **Dependence of the hydrodynamic radius of apoflavodoxin-A488 on concentration of GuHCl as determined by FCS measurements.** *A*, relative hydrodynamic radius of apoflavodoxin at different GuHCl concentrations (errors are within ±8%). Each *data point* is the result of linking parameters of five separate FCS measurements in the fitting procedure (see "Experimental Procedures"). As a visual aid, a fit of a two-state unfolding model to the data is shown. *B*, fractions of native (*N*), intermediate (*I*), and unfolded (*U*) states of apoflavodoxin as a function of GuHCl concentration (27).

account the known dependence of the fractions of folding species involved on the concentration of denaturant (Fig. 1*B*) (27). For example, at 2 M GuHCl, 53% of the apoflavodoxin molecules are off-pathway folding intermediate, 46% are unfolded, and only 2% of the protein molecules are native. Consequently, using a hydrodynamic radius of 38 Å for the unfolded state and 28 Å for the native state, it is estimated that the intermediate species has an average hydrodynamic radius of ~31 Å. Thus, the radius of apoflavodoxin expands by about 11% upon going from native to molten globule-like state at 2 M GuHCl (*i.e.* a 36% increase in volume). Indeed, the molten globule-like species observed during apoflavodoxin folding is relatively compact.

Crowding Does Not Affect the Conformation of Native Apoflavodoxin—Since the hydrodynamic radii of the native, intermediate, and unfolded states of apoflavodoxin are not the same, it is expected that macromolecular crowding will affect these states differently. Intrinsic tryptophan fluorescence (Fig. 2) and circular dichroism (Fig. 3) were used to detect potential influences of crowding on the three folding states of apoflavodoxin. Crowded conditions were created by the presence of dextran 20 to 30% (w/v), since this condition mimics the crowded circumstances in the cytoplasm of *E. coli* cells rather well (4).

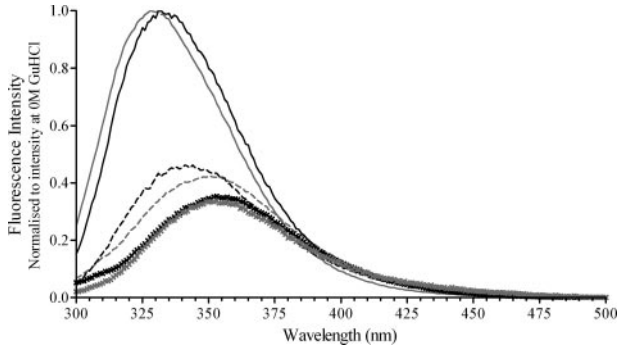

FIGURE 2. **Tryptophan fluorescence spectra of apoflavodoxin in the absence and presence of macromolecular crowders.** Spectra of apoflavodoxin at 0 M (*solid lines*, native protein), 2 M (*dashes*), and 3 M GuHCl (+) are shown in the absence (*gray lines*) and presence (*black lines*) of 30% (w/v) dextran 20. The addition of dextrans causes a slight loss in fluorescence emission intensity of the protein. The spectra shown are corrected for this intensity loss. The protein concentration in all samples is 2 μM.

The addition of dextran 20 caused scattering as well as absorption of excitation light, and as a result, a slight decrease in fluorescence intensities of all three folding states was observed (data not shown). The presence of dextran 20 at 30% (w/v) also caused a red shift of the emission maximum by ~4 nm due to scattering, as shown for native protein in Fig. 2. Far-UV CD spectra show that the secondary structure content of native apoflavodoxin did not alter due to macromolecular crowding (Fig. 3*A*). In addition, the presence of dextran 20 did not lead to a change in the near-UV CD spectrum of native protein, showing that the tertiary structure of native apoflavodoxin was also unaffected by dextran 20 (Fig. 3*C*). Both observations show that crowding does not affect the conformation of native apoflavodoxin. This conclusion was further supported by FRET measurements using dye-labeled apoflavodoxin molecules, as is shown below.

Crowding Causes Aggregation of the Molten Globule-like Folding Intermediate of Apoflavodoxin—Fluorescence emission spectra of proteins are particularly sensitive to alterations in the local microenvironment of tryptophans. The addition of 2 or 3 M GuHCl to native apoflavodoxin changed the corresponding fluorescence emission spectrum (Fig. 2). This change was due to protein unfolding and consequent population of intermediate and unfolded states of apoflavodoxin. The fluorescence emission of both of these nonnative states was severely quenched and shifted to longer wavelengths compared with fluorescence emission of native apoflavodoxin. These effects were caused by solvent exposure of the three tryptophans of apoflavodoxin in these folding species (27).

At 2 M GuHCl, 53% of apoflavodoxin molecules were folding intermediates, and virtually all other protein molecules were unfolded (Fig. 1*B*). Under these denaturing conditions, the addition of dextran 20 to 30% (w/v) caused the fluorescence emission maximum to shift to the blue by ~6 nm, and also a slight increase in fluorescence intensity was observed (Fig. 2). In addition, the far-UV CD spectrum showed that the ellipticity at 222 nm became more negative (Fig. 3*A*). These changes in fluorescence emission and far-UV CD were most likely caused by an increased percentage of native and

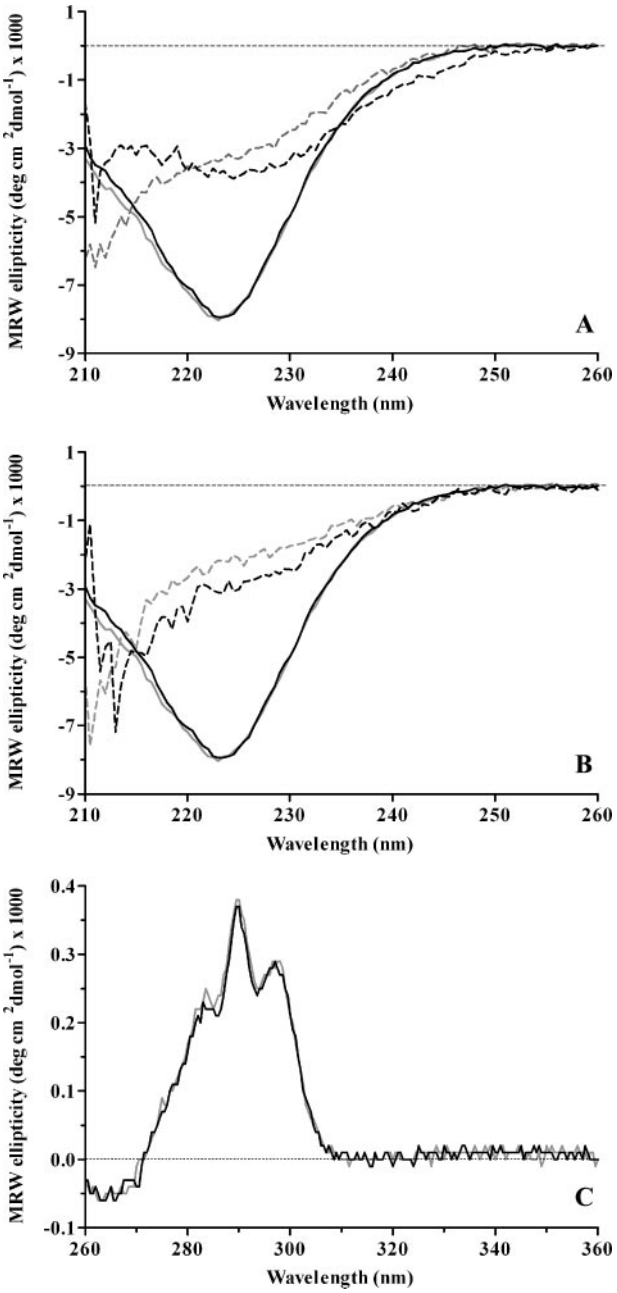

FIGURE 3. **Far- and near-UV CD spectra of apoflavodoxin in the absence and presence of macromolecular crowders.** *A*, far-UV CD spectra of apoflavodoxin in 2 M GuHCl in the absence (*dashed gray line*) and presence (*dashed black line*) of 30% (w/v) dextran 20. MRW, mean residue weight. *B*, far-UV CD spectrum of apoflavodoxin in 3 M GuHCl in the absence (*dashed gray line*) and presence (*dashed black line*) of 30% (w/v) dextran 20. *Solid lines* in *A* and *B* show the far-UV CD spectra of native apoflavodoxin in the absence (*gray*) and presence (*black*) of 40% (w/v) dextran 20. *C*, near-UV CD spectra of native apoflavodoxin in the absence (*gray lines*) and presence (*black lines*) of 40% (w/v) dextran 20. Protein concentration is 4 μM (far-UV CD) or 23.5 μM (near-UV CD).

molten globule-like protein molecules as crowding stabilizes folded structures.

Fluorescence measurements show that the transition zone of GuHCl-induced apoflavodoxin unfolding coincides with the one obtained for refolding, showing that apoflavodoxin unfolding is fully reversible up to 6 μM protein concentration (25, 27). This feature was exploited to investigate whether apoflavodoxin unfolding in the presence of dextran 20 was also reversible. Protein unfolded in 2 M GuHCl (protein concentration 2 μM) in the presence of 30% (w/v) dextran 20 was diluted 10-fold through the addition of buffer that also contained 30% (w/v) dextran 20. The recovery, in terms of percentage of fluorescence intensity, compared with the recovery in a fully reversible refolding experiment in which no crowding agent was present was 25% (Fig. 4). In a similar experiment in the continuous presence of 40% (w/v) dextran 20, recovery was only 10% (Fig. 4). Centrifugation of a sample of apoflavodoxin molecules at 2 M denaturant in the presence of 30% (w/v) dextran 20 produced a protein pellet showing that this nonreversibility was due to protein aggregation. Without dextran 20, no protein aggregation was observed even in a solution that contained twice as much apoflavodoxin at 2 M GuHCl. At 2 M denaturant, the molten globule-like intermediate, which has exposed hydrophobic residues, like tryptophans, is populated to a high level. It is likely that this species caused the observed protein aggregation.

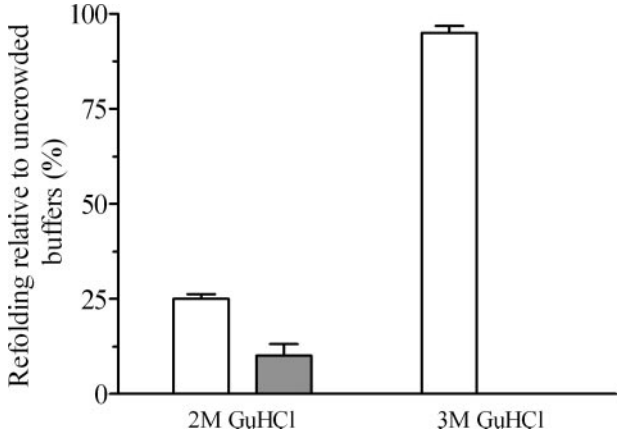

FIGURE 4. **Reversibility of GuHCl-induced unfolding of native apoflavodoxin in the presence of crowders.** Protein (2 μM) unfolded at 2 M or 3 M GuHCl is refolded by dilution of the denaturant to ≤1 M GuHCl in the continuous presence of 30% (w/v) (*white bar*) or 40% (w/v) (*gray bar*) dextran 20. The *bars* show the recovery in terms of percentage of fluorescence intensity at 340 nm averaged over a period of 30 s compared with recovery in a fully reversible refolding experiment in which no crowding agent is present. S.E. values are shown.

Crowding Causes Compaction of Unfolded Apoflavodoxin—To investigate the impact of crowding on the unfolded state, this state was populated by the addition of GuHCl. At 3 M GuHCl, unfolded apoflavodoxin is the dominating species, since 95% of protein molecules populate this state, and the remaining percentage represents folding intermediate (Fig. 1*B*). Due to limitations in solubility, the concentration of GuHCl cannot exceed 3 M in the presence of 30% (w/v) dextran 20. At 3 M GuHCl, the addition of dextran 20 to 30% (w/v) did not significantly alter the fluorescence emission spectrum of the protein (Fig. 2). Next, the reversibility of protein unfolding at 3 M GuHCl in the presence of crowding agent was investigated using fluorescence emission. Unfolded apoflavodoxin at 3 M GuHCl in the presence of 30% (w/v) dextran 20 was diluted 10-fold through the addition of buffer that also contained 30% (w/v) dextran 20. This led to full recovery of the native state (Fig. 4). Thus, in contrast to what was observed for protein unfolded in 2 M GuHCl, apoflavodoxin unfolding was fully reversible upon refolding the protein from 3 M GuHCl, at which

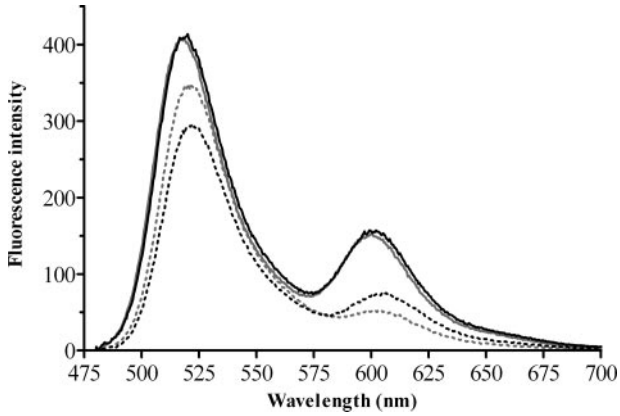

FIGURE 5. **Donor and acceptor fluorescence intensities of dye-labeled native and unfolded apoflavodoxin in the absence and presence of macromolecular crowders.** The protein is labeled with A488 at position 69 and with A568 at position 178. The *solid lines* show fluorescence spectra of native apoflavodoxin in the absence (*gray*) and in the presence (*black*) of 30% (w/v) dextran-20. The *dashed lines* show fluorescence spectra of unfolded apoflavodoxin in 3 M GuHCl in the absence (*gray*) and in the presence (*black*) of 30% (w/v) dextran 20. The addition of dextrans causes a slight loss in fluorescence emission intensity of the protein. The spectra shown are corrected for this intensity loss. Protein concentration is 84 nM.

concentration of denaturant the aggregation-prone folding intermediate is hardly populated.

At 3 M GuHCl, the addition of dextran 20 to 30% (w/v) caused the far-UV CD ellipticity values of apoflavodoxin to become more negative (Fig. 3*B*), indicating increased formation of secondary structure in the unfolded protein. This increased secondary structure content could lead to a decrease in average dimensions of unfolded molecules. FCS did not detect changes in the hydrodynamic radius of unfolded protein at 3 M GuHCl due to the addition of 30% (w/v) dextran 20 (data not shown). Since hydrodynamic radii determined by FCS are associated with relatively large errors (~8%), small changes potentially induced by crowding in the overall dimension of the unfolded protein were missed.

FRET is sensitive to changes on the nanometer scale; therefore, it was chosen to study the effect of crowding on the dimensions of unfolded apoflavodoxin. To enable this FRET study, a double cysteine variant of wild-type apoflavodoxin was generated through replacement of Ser-178 with a cysteine. The resulting protein variant was labeled with A488 as donor at position Cys-69 and with A568 as acceptor at position Cys-178. This protein variant has similar stability as wild-type apoflavodoxin, and labeling with A488 and A568 affected the stability only marginally (details of the dye labeling procedure will be published elsewhere). Cysteine residues 69 and 178 are positioned on diametrically opposite sides of the native protein (22).

In the case of native apoflavodoxin, the addition of 30% (w/v) dextran 20 did not alter the FRET efficiency (*E*) significantly. For protein in buffer, *E* was 0.55 ± 0.01, and for protein in buffer containing 30% (w/v) dextran, *E* was 0.53 ± 0.01, giving a distance between dyes (*R*) of 51.4 ± 0.5 and 51.0 ± 0.5 Å, respectively. Thus, the measurements confirm that macromolecular crowding does not affect the conformation of native apoflavodoxin. Upon unfolding apoflavodoxin through the addition of 3 M GuHCl, the FRET efficiency between both attached chromophores was reduced to 0.30 ± 0.01 (Fig. 5).

TABLE 1

Changes in thermal unfolding midpoint of apoflavodoxin due to macromolecular crowding

Thermal unfolding parameters were obtained by fitting Equations 8 and 9 to temperature-dependent fluorescence emission data of 2 μM apoflavodoxin (see "Experimental Procedures"). For native apoflavodoxin in buffer without crowding agents, the following parameters were obtained: $T_{m,\ buffer}$ = 48.1 ± 0.1 °C, ΔH_m = 76.8 ± 0.9 kcal mol^{-1}, and ΔC_p = 1.3 ± 0.7 kcal mol^{-1}K^{-1}. In the presence of dextrans, thermal unfolding curves are obtained that could be fitted with values of ΔH_m and ΔC_p that are similar within S.E. to the values mentioned above. $T_{m,\ crowded}$ is the T_m obtained for apoflavodoxin in the presence of dextran.

Crowding agent	Concentration	$\Delta T_m = T_{m,\ crowded} - T_{m,\ buffer}$
	% (w/v)	*°C*
Dex-06	40	4.2 ± 0.3
Dex-20	30	2.9 ± 0.1
Dex-20	40	3.8 ± 0.2
Dex-70	40	4.2 ± 0.2

Such reduction is expected, since upon protein unfolding, the distance between donor and acceptor increases. In the presence of 30% (w/v) dextran 20, however, the FRET efficiency measured for unfolded apoflavodoxin was clearly higher (*i.e.* 0.40 ± 0.01) than in the absence of crowding agent (*i.e.* 0.30 ± 0.01). This observation implies that crowding causes the distance between donor and acceptor dyes attached to unfolded apoflavodoxin to become smaller. A change in the FRET efficiency from 0.30 to 0.40 means that the distance between the labels changes from 59.9 ± 0.7 Å in the unfolded state, in the absence of dextran 20, to 54.0 ± 0.6 Å in the presence of dextran 20. This 5.9 ± 0.9 Å reduction in distance, taken together with the observation that the addition of dextran 20 to 30% (w/v) caused the far-UV CD ellipticity values at 222 nm of unfolded apoflavodoxin to become more negative (see Fig. 3*B*), implies increased structure formation between residues 69 and 178 of the unfolded protein. Alternatively, these results could also be partially due to an increase in the population of the intermediate state of apoflavodoxin. The addition of dextran 20 to 30% (w/v) to unfolded apoflavodoxin in 3 M GuHCl led to a decrease in protein volume of about 29%.

Macromolecular Crowding Stabilizes Apoflavodoxin against Thermal Unfolding—Compaction of the unfolded state due to macromolecular crowding implies that both native apoflavodoxin and the off-pathway folding intermediate gains extra stability against unfolding. This stability increase was studied by thermal denaturation of apoflavodoxin as monitored with intrinsic tryptophan fluorescence. The fluorescence intensity decreased upon thermal unfolding of apoflavodoxin as the population of the highly fluorescent native state diminished and the population of nonnative apoflavodoxin folding states, which have severely quenched fluorescence, increased. Table 1 shows that the addition of 30% (w/v) dextran 20 to a 2 μM protein solution caused an increase of 2.9 °C in thermal midpoint (T_m) of apoflavodoxin unfolding. Raising dextran 20 to 40% (w/v) led to a further 1.3 °C increase in T_m. These observations show that macromolecular crowding increases the stability of native apoflavodoxin against unfolding.

When 2 μM apoflavodoxin was unfolded by gradually raising the temperature to 65 °C and subsequently refolded by gradually lowering the temperature to 25 °C, only 60% of native state fluorescence intensity was recovered (Fig. 6). Repeating this experiment in the presence of 30% (w/v) dextran 20 led to a

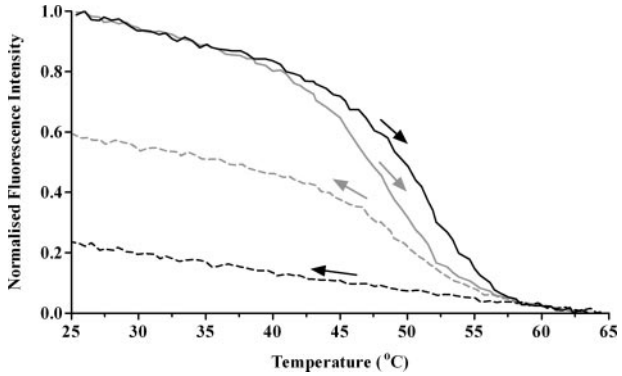

FIGURE 6. **Effect of macromolecular crowding on the stability of apoflavodoxin against thermal unfolding as monitored by the change in fluorescence emission at 340 nm.** Thermal unfolding (*solid lines*) and subsequent refolding (*dashed lines*) experiments are performed in the presence (*black*) and in the absence (*gray*) of 30% (w/v) dextran 20. The *arrows pointing* to the *right* show the heating trajectories, and *arrows pointing* to the *left* show the subsequent cooling trajectories. The excitation wavelength is 280 nm, the protein concentration is 2 μM, and the heating rate is 0.5 °C/min.

recovery of only 20% of native state fluorescence intensity (Fig. 6). Both apoflavodoxin samples also showed a visible increase in turbidity as the protein was heated. Formation of large protein particles during thermal unfolding was inferred from light scattering measurements monitored at 560 nm (data not shown). These observations demonstrate that protein aggregation is strongly promoted due to the presence of high concentrations of dextran 20.

Aggregation during the measurement of a thermal unfolding curve can affect T_m. When the rate of protein aggregation during thermal unfolding becomes sufficiently large ($k_{\text{aggregation}} > \sim 0.1\ \text{min}^{-1}$), the apparent T_m value determined becomes lower than the actual value of T_m that is associated with protein stability (51, 52). To resolve whether this phenomenon occurs during apoflavodoxin unfolding, the effects of different aggregation conditions on T_m were investigated. First, the effect of raising the protein concentration in a noncrowded solution was studied. Upon increasing apoflavodoxin concentration 200-fold, recovery of native state fluorescence intensity in a thermal unfolding/refolding experiment decreased due to enhanced aggregation from 75% at 0.5 μM protein concentration to only 12% at 100 μM protein concentration. However, the corresponding T_m values were unaffected within error (data not shown). Second, the influence of increasing the heating rate on T_m in crowded and noncrowded solutions was studied. At a larger heating rate, less time is available for aggregation to influence a thermal unfolding/refolding experiment. A recovery of 70% of native state fluorescence was obtained using heating and cooling rates of 1.5 or 3 °C/min and a 2 μM protein solution without dextran 20. However, both in the presence and absence of dextran 20, increasing the heating rate from 0.5 to 3 °C/min did not affect T_m (data not shown). Finally, the viscosity of the solution was altered through the addition of dextrans of different average molecular masses (*i.e.* dextran 06, dextran 20, or dextran 70) at 40% (w/v) concentration. The crowding effects of these dextrans, at the same weight/volume concentrations, were exclusively determined by their cylindrical radii, which were identical (Equation 11). Since increasing the molecular weight of the dextran involved causes the viscosity of the solution to become larger, aggregation will proceed slower during a thermal unfolding/refolding experiment (53). Table 1 shows that despite viscosity-induced changes in the rate of aggregation, T_m was not affected within error.

Clearly, enhancing the rate of protein aggregation due to altering protein concentration, heating rate, or viscosity of the solution did not lower the apparent T_m value of apoflavodoxin. In addition, the presence of dextran enhanced aggregation severely, but instead of lowering T_m, macromolecular crowding caused a significant increase in the thermal midpoint of apoflavodoxin (Table 1). These observations imply that the rate of protein aggregation during thermal unfolding of apoflavodoxin must be lower than $\sim 0.1\ \text{min}^{-1}$ under all experimental circumstances investigated (51, 54). Consequently, the observed increase in T_m of apoflavodoxin due to the addition of dextran truly reflects a crowding-induced stability enhancement of the protein. Indeed, the addition of three differing crowding agents with similar crowding effects (*i.e.* dextran 06, dextran 20, or dextran 70 at 40% (w/v)) to apoflavodoxin led to a comparable increase in the thermal midpoint of apoflavodoxin unfolding (Table 1).

DISCUSSION

To understand folding in the densely crowded cellular milieu, it is necessary to experimentally test the effects of crowding on the intrinsic features of protein folding. Here, the effect of macromolecular crowding on apoflavodoxin from *A. vinelandii* was investigated, and it is shown that crowding does influence apoflavodoxin folding *in vitro*.

FCS was used to follow changes in hydrodynamic radius of apoflavodoxin upon its denaturant-induced unfolding. The FCS data show that native apoflavodoxin has a hydrodynamic radius of 28 ± 1 Å, and upon formation of the molten globule-like folding intermediate at 2 M GuHCl, the protein radius increases by about 11%. Far- and near-UV CD spectroscopy and FRET measurements of dye-labeled apoflavodoxin show that the conformation of native apoflavodoxin is not detectably altered due to crowding. Whether crowding-induced compaction of the folding intermediate occurs could not be revealed, since aggregation affects the data obtained at the denaturant concentration at which this state is significantly populated (*i.e.* at about 2 M GuHCl).

In a recent study of apoflavodoxin from *Desulfovibrio desulfuricans*, it was claimed that macromolecular crowding causes an apparent increase in secondary structure of the native protein as judged by far-UV circular dichroism (55). It was stated that crowder Ficoll 70 compacts native apoflavodoxin and causes the helical content of the native protein to rise up to 20% in 10 mM Hepes, at 20 °C, and similar trends were apparently observed for native holoflavodoxin (55). However, this increase in helical content and associated molecular compaction is improbable, since structural studies convincingly show that the native conformation of apoflavodoxin is virtually identical to that of holoflavodoxin, which is densely packed and compact (32, 56). Native apo- and holoflavodoxin molecules can hardly be reduced in volume.

In contrast to other apoflavodoxins, the stability of *D. desulfuricans* apoflavodoxin is very sensitive to buffer composition.

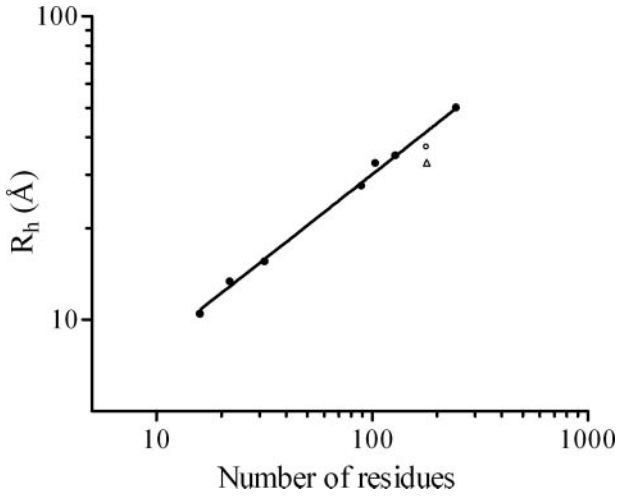

FIGURE 7. **Hydrodynamic radii of various chemically denatured proteins *versus* number of residues.** Data from proteins (●) other than apoflavodoxin from *A. vinelandii* are taken from Wilkins *et al.* (58). Errors in hydrodynamic radii are within ±3%. The *solid line* is the result of the fit of a linear equation to the data. The hydrodynamic radius of the 179-residue apoflavodoxin at 3 M GuHCl is derived from FCS data (○). FRET data of dye-labeled apoflavodoxin molecules show that the subsequent addition of 30% (w/v) dextran 20 leads to compaction of unfolded apoflavodoxin by about 10% (△).

Its thermal midpoint of unfolding can decrease as much as 25 °C upon changing from phosphate to Hepes buffer, which corresponds to an exceptionally large protein destabilization (55). The addition of Ficoll 70 increases T_m maximally by 20 °C, as shown by far-UV circular dichroism (55). Using the corresponding ΔH_m (57) and estimated ΔC_p of 2.5 kcal mol^{-1} K^{-1}, the stability of apoflavodoxin in 10 mM Hepes is calculated to be maximally 1.5 kcal mol^{-1}. Application of Boltzmann's distribution function shows that about 8% of all apoflavodoxin molecules are unfolded under these conditions. Protein stability increases modestly upon adding Ficoll 70 (16) and tips the balance between unfolded and native *D. desulfuricans* apoflavodoxin molecules further toward native ones. This general phenomenon causes the reported increase in far-UV CD signal. Consequently, secondary structure content of this native protein seems to rise. Since native *A. vinelandii* apoflavodoxin has a relatively large stability of 10.45 kcal mol^{-1} (27) under the conditions used in this study, only a negligible fraction of protein molecules (about 0.000002%) is in the unfolded state. Hence, the addition of dextran 20 cannot detectably increase the population of native apoflavodoxin molecules. Consequently, since upon crowding no change in the far- and near-UV CD signals of native apoflavodoxin is experimentally observed, crowding does not detectably affect the conformation of native *A. vinelandii* apoflavodoxin.

At 3 M GuHCl, the maximum concentration of denaturant to which dextran 20 can be added to 30% (w/v), FCS shows that unfolded apoflavodoxin has a hydrodynamic radius of 37 ± 3 Å (Fig. 1). This value is within error similar to the hydrodynamic radius of 38 ± 4 Å of the protein at 4 M GuHCl, where it is fully denatured (27). Compared with hydrodynamic radii of other chemically denatured proteins (58), these values fall well within the range of radii expected for a random coil of 179 residues (Fig. 7). FRET measurements show that the addition of 30% (w/v) dextran 20 to apoflavodoxin in 3 M GuHCl causes compaction of the unfolded state (Fig. 5). The average distance between the dye labels decreases by ~10%. If the hydrodynamic radius of the protein would also decrease by 10%, using the FCS data of the unfolded protein in absence of crowding agents as reference state, we calculate that the hydrodynamic radius of the unfolded protein decreases from 37 Å to about 33 Å (Fig. 7). Far-UV CD spectroscopy shows that compaction of the unfolded state is accompanied by a concomitant increase in secondary structure content. The observed reduction in FRET efficiency due to the addition of crowding agents at 3 M GuHCl could be caused by a slight increase in population of the intermediate folding state, which is rather compact and structured or due to structure formation in unfolded state, or it could be caused by a combination of the two. It might be possible that the decrease in average radius of the unfolded protein upon adding 30% (w/v) dextran deviates from 10%, the value derived from FRET measurements using a two-point analysis. Nevertheless, our data (FRET, far-UV CD, and thermal unfolding experiments) show that unfolded apoflavodoxin compacts upon macromolecular crowding. Crowding destabilizes the unfolded state of apoflavodoxin, and thus the stability of the native and intermediate folding species against unfolding increases.

The change in free energy difference (ΔG) between native and unfolded apoflavodoxin upon the addition of dextran 20, under the experimental conditions investigated, can be estimated. The excluded volume effect of dextran is estimated using the "equivalent hard particle model" (12, 17). The reduction in the average hydrodynamic radius of unfolded apoflavodoxin at 3 M GuHCl by ~10% due to the presence of 30% (w/v) dextran 20 destabilizes the unfolded state of apoflavodoxin by maximally 1.1 kcal mol^{-1}. This destabilization is most likely an overestimation of the true stability increase (see the Appendix). The net result is that crowding stabilizes native apoflavodoxin against unfolding by maximally 1.1 kcal mol^{-1}.

The crowding-induced increase in stability of native apoflavodoxin is relatively small compared with the 10.45 kcal mol^{-1} that is required to unfold native protein in the absence of dextran 20 (27). Similar crowding-induced stability changes, which vary from insignificant to ~2.9 kcal mol^{-1}, have been observed for other proteins in similarly crowded conditions (11, 12, 16). Indeed, the addition of 30% (w/v) dextran 20 leads to a marginal increase of 2.9 °C in the thermal midpoint of apoflavodoxin (Table 1). The addition of dextran 06, dextran 20, or dextran 70 to 40% (w/v) increases T_m of apoflavodoxin by about 4 °C (Table 1). This increase in T_m due to crowding is in the range of what has been observed for lysozyme and cytochrome *c* and of what has been predicted for various eukaryotic proteins (9, 12, 14). Although the effect of crowding on protein stability is rather limited, the crowding-induced compaction of unfolded apoflavodoxin in which secondary structure is formed shows that crowding restricts the conformational space sampled by the unfolded state.

In a noncrowded solution that contains 6 μM apoflavodoxin, no aggregation of the intermediate species is observed at 2 M GuHCl, and protein unfolding is fully reversible. In crowded solutions, the thermodynamic activity of the protein is predicted to increase dramatically, thereby enhancing aggregation

rates by several orders of magnitude (17). In a solution that is crowded due to the presence of 30% (w/v) dextran 20, the thermodynamic activity of apoflavodoxin unfolded in 2 M GuHCl is up to 3 orders of magnitude higher than in the corresponding noncrowded solution (see the Appendix). Under these circumstances, aggregation of molten-globule like folding species, which are partially folded and can form aggregates via specific interactions between structured elements (59–63), is promoted. Crowding also increases solvent viscosity, and this lowers the collision frequency of protein molecules (2). FCS data show that the addition of 30% (w/v) dextran 20 leads to about 10-fold lowering of the diffusion coefficient of apoflavodoxin (data not shown). Since the collision rate of protein molecules is proportional to their diffusion coefficients, this rate also drops about 10-fold. However, this effect is by far outweighed by the ~1000-fold increase in effective protein concentration due to the addition of 30% (w/v) dextran 20. Consequently, under these crowded circumstances, aggregation of the molten globule-like folding intermediate of apoflavodoxin is strongly promoted.

Although protein folding *in vivo* can be influenced by many specific and nonspecific interactions of the folding polypeptide chain with other cellular components, it is expected that macromolecular crowding remains a major factor that affects protein folding (64, 65). This study demonstrates that crowding destabilizes unfolded apoflavodoxin, which becomes more compact and also acquires secondary structure. In addition, crowding causes severe aggregation of the off-pathway intermediate of apoflavodoxin. What could be the implications of these observations for flavodoxin folding *in vivo*?

Compaction of unfolded apoflavodoxin due to macromolecular crowding can potentially affect kinetic folding of apoflavodoxin, since it restricts the conformational space sampled by the unfolded protein. The prediction that compact (native) states are stabilized under crowded conditions relative to less compact partially folded or unfolded states suggests that crowding could alter the free energy landscape of protein folding significantly (18). Macromolecular crowding can indeed accelerate folding steps that involve structural collapse and decelerate folding steps that involve local unfolding of intermediates, as shown by experiment (66) and theory (67). It is thus likely that under circumstances that mimic the intracellular environment, the rates associated with apoflavodoxin folding processes are altered compared with those observed in dilute solutions.

One of the most important consequences of crowding is that intermolecular interactions become strongly favored. Indeed, in this study, severe aggregation of partially folded apoflavodoxin molecules is observed in crowded solutions. Inside a cell, ample opportunities exist for aggregation of partially folded apoflavodoxin chains (64, 68). This nonproductive aggregation can compete with productive folding. However, flavodoxin is overexpressed in the cytoplasm of *E. coli* and folds to its native functional form at high yield without noticeable problems (41).

In *E. coli*, Trigger Factor is the first chaperone to meet nascent apoflavodoxin molecules as they emerge from the ribosome (68, 69). Residues 45–60 of nascent apoflavodoxin constitute a hydrophobic region in the core of the native protein, and this region probably interacts with Trigger Factor. This chaperone could thus prevent nascent apoflavodoxin chains from aggregating with partially folded protein molecules, which can be other nascent apoflavodoxin molecules that are formed by a polyribosome. Subsequent to Trigger Factor, chaperone DnaK can bind to nascent apoflavodoxin. Indeed, in apoflavodoxin, five high affinity recognition motifs for chaperone DnaK are predicted using the algorithm developed by Rüdiger *et al.* (70). In a proteome-wide analysis of chaperonin-dependent protein folding in *E. coli*, it is found that flavodoxin from *E. coli* has no obligate requirement for chaperonin GroEL (71). Apparently, the presence of Trigger Factor and the DnaK system (*i.e.* DnaK, DnaJ, and GrpE) is sufficient to avoid aggregation of folding apoflavodoxin molecules and to enhance production of native protein molecules in the crowded intracellular milieu of *E. coli*.

How crowding alters apoflavodoxin folding kinetics and corresponding folding energy landscape and how chaperones influence apoflavodoxin folding will be subjects of future studies.

APPENDIX

Estimation of the Stability Increase of Apoflavodoxin Due to Macromolecular Crowding Using the "Equivalent Hard Particle" Model for the Excluded Volume Effect of Dextran

The thermodynamic activity a_i of protein P_i (where i denotes a particular protein conformation) is related to its concentration c_i via activity coefficient γ_i.

$$a_i = \gamma_i \cdot c_i \qquad \text{(Eq. 10)}$$

In the case of globular proteins that can be modeled as rigid spheres, the natural logarithm of γ_i can be defined as follows (72),

$$\ln \gamma_i = (1 + r_i/r_b)^2 \cdot \nu_b \cdot w_b \qquad \text{(Eq. 11)}$$

where r_i represents the spherical radius of protein species i, r_b is the cylindrical radius of crowding agent b, ν_b is the specific excluded volume occupied by b, and w_b is the concentration of b in weight/volume units. For dextran, $r_b = 7$ Å (12, 73), and $\nu_b = 0.0008$ liter · gram^{-1} (35).

In crowded solutions, the thermodynamic activity of the protein is predicted to increase dramatically, thereby enhancing aggregation rates by several orders of magnitude. In the presence of 2 M GuHCl, the average hydrodynamic radius of apoflavodoxin, r_{2M} is 34 Å (extracted from FCS data; Fig. 1). Assuming that this radius does not change significantly by the addition of 30% (w/v) dextran 20, a_{2M} for 2 μM apoflavodoxin is calculated to be 7 mM.

In solutions crowded with macromolecules, the volume available to a particular protein molecule is reduced compared with that in noncrowded solutions. Thus, crowding causes a decrease of the configurational entropy of the protein species involved, and as a result, its chemical potential increases relative to that in dilute solution. The thermodynamic activity coefficient γ_i is used to calculate this excess chemical potential, μ_i^{ex},

of a particular protein species P_i due to macromolecular crowding (17),

$$\mu_i^{ex} = RT\ln \gamma_i \quad \text{(Eq. 12)}$$

where $R = 1.987$ cal K^{-1} mol^{-1}, the molar gas constant and T is the temperature in Kelvin.

In the presence of 30% (w/v) dextran 20, the hydrodynamic radius r_N of native apoflavodoxin is 28 Å (extracted from FCS and FRET data). The protein concentration used is 2 μM, and consequently $\ln \gamma_N = 6$ and thus $a_N = 0.8$ mM. Crowding raises the chemical potential of native apoflavodoxin by 3.5 kcal mol^{-1}. In the unlikely situation that unfolded apoflavodoxin has the same hydrodynamic radius as native apoflavodoxin, crowding by 30% (w/v) dextran 20 also causes the chemical potential of unfolded apoflavodoxin to rise by 3.5 kcal mol^{-1}. Thus, no effect of crowding on the thermal midpoint of apoflavodoxin unfolding would be observed. Experimentally, this situation is clearly not observed, since T_m increases upon the addition of crowding agents (Table 1). Consequently, unfolded apoflavodoxin must have a hydrodynamic radius that is larger than 28 Å. Indeed, in the presence of 30% (w/v) dextran 20, the hydrodynamic radius of apoflavodoxin at 3 M GuHCl is estimated to be 33 Å (derived from FCS data taking into account a reduction of 10% in the hydrodynamic radius in crowded solution as implied by the FRET results). Suppose that the hydrodynamic radius of the unfolded protein in the absence of denaturant but in the presence of 30% (w/v) dextran 20 is also 33 Å. In this situation, the calculated value of $\ln \gamma_U = 7.8$, and thus a_U is 5 mM. Now crowding causes a 4.6 kcal mol^{-1} rise in chemical potential of unfolded apoflavodoxin. As a result, the crowding-induced increase in free energy difference between native and unfolded apoflavodoxin is calculated to be 1.1 kcal mol^{-1}. The latter value is almost certainly an overestimation of the true crowding-induced change in stability of apoflavodoxin due to the following reasoning. The hydrodynamic radius of unfolded apoflavodoxin in the absence of denaturant will be smaller than 33 Å, since upon removal of denaturant, unfolded protein molecules collapse (74).

REFERENCES

1. Anfinsen, C. B. (1973) *Science* **181,** 223–230
2. Ellis, R. J. (2001) *Curr. Opin. Struct. Biol.* **11,** 114–119
3. Luby-Phelps, K. (2000) *Int. Rev. Cytol.* **192,** 189–221
4. Zimmerman, S. B., and Trach, S. O. (1991) *J. Mol. Biol.* **222,** 599–620
5. Minton, A. P. (2006) *J. Cell Sci.* **119,** 2863–2869
6. Ellis, R. J. (2001) *Trends Biochem. Sci.* **26,** 597–604
7. Zimmerman, S. B., and Minton, A. P. (1993) *Annu. Rev. Biophys. Biomol. Struct.* **22,** 27–65
8. Minton, A. P. (2005) *Biophys. J.* **88,** 971–985
9. Despa, F., Orgill, D. P., and Lee, R. C. (2005) *Ann. N. Y. Acad. Sci.* **1066,** 54–66
10. Minton, A. P. (2005) *J. Pharmacol. Sci.* **94,** 1668–1675
11. Qu, Y. X., and Bolen, D. W. (2002) *Biophys. Chem.* **101,** 155–165
12. Sasahara, K., McPhie, P., and Minton, A. P. (2003) *J. Mol. Biol.* **326,** 1227–1237
13. Tokuriki, N., Kinjo, M., Negi, S., Hoshino, M., Goto, Y., Urabe, I., and Yomo, T. (2004) *Protein Sci.* **13,** 125–133
14. Hall, D., and Dobson, C. M. (2006) *FEBS Lett.* **580,** 2584–2590
15. McPhie, P., Ni, Y., and Minton, A. P. (2006) *J. Mol. Biol.* **361,** 7–10
16. Spencer, D. S., Xu, K., Logan, T. M., and Zhou, H.-X. (2005) *J. Mol. Biol.* **351,** 219–232
17. Ellis, R. J., and Minton, A. P. (2006) *Biol. Chem.* **387,** 485–497
18. Minton, A. P. (2000) *Curr. Opin. Struct. Biol.* **10,** 34–39
19. Du, F., Zhou, Z., Mo, Z. Y., Shi, J. Z., Chen, J., and Liang, Y. (2006) *J. Mol. Biol.* **364,** 469–482
20. Martin, J. (2002) *Biochemistry* **41,** 5050–5055
21. van den Berg, B., Ellis, R. J., and Dobson, C. M. (1999) *EMBO J.* **18,** 6927–6933
22. Alagaratnam, S., van Pouderoyen, G., Pijning, T., Dijkstra, B. W., Cavazzini, D., Rossi, G. L., Van Dongen, W. M., van Mierlo, C. P., van Berkel, W. J., and Canters, G. W. (2005) *Protein Sci.* **14,** 2284–2295
23. Sancho, J. (2006) *Cell. Mol. Life Sci.* **63,** 855–864
24. van Mierlo, C. P. M., and Steensma, E. (2000) *J. Biotechnol.* **79,** 281–298
25. van Mierlo, C. P., van Dongen, W. M. A. M., Vergeldt, F., Van-Berkel, W. J. H., and Steensma, E. (1998) *Protein Sci.* **7,** 2331–2344
26. van Mierlo, C. P., van den Oever, J. M., and Steensma, E. (2000) *Protein Sci.* **9,** 145–157
27. Bollen, Y. J., Sanchez, I. E., and van Mierlo, C. P. (2004) *Biochemistry* **43,** 10475–10489
28. Bollen, Y. J., Nabuurs, S. M., van Berkel, W. J., and van Mierlo, C. P. (2005) *J. Biol. Chem.* **280,** 7836–7844
29. Bollen, Y. J., and van Mierlo, C. P. (2005) *Biophys. Chem.* **114,** 181–189
30. Bollen, Y. J. M., Kamphuis, M. B., and van Mierlo, C. P. M. (2006) *Proc. Natl. Acad. Sci. U. S. A.* **103,** 4095–4100
31. Steensma, E., Nijman, M. J., Bollen, Y. J., de Jager, P. A., van den Berg, W. A., van Dongen, W. M., and van Mierlo, C. P. (1998) *Protein Sci.* **7,** 306–317
32. Steensma, E., and van Mierlo, C. P. M. (1998) *J. Mol. Biol.* **282,** 653–666
33. Laurent, T. C. (1963) *Biochem. J.* **89,** 253–257
34. Rivas, G., Fernandez, J. A., and Minton, A. P. (1999) *Biochemistry* **38,** 9379–9388
35. Hatters, D. M., Minton, A. P., and Howlett, G. J. (2002) *J. Biol. Chem.* **277,** 7824–7830
36. Jarvis, T. C., Ring, D. M., Daube, S. S., and von Hippel, P. H. (1990) *J. Biol. Chem.* **265,** 15160–15167
37. Lindner, R. A., and Ralston, G. B. (1995) *Biophys. Chem.* **57,** 15–25
38. Lindner, R. A., and Ralston, G. B. (1997) *Biophys. Chem.* **66,** 57–66
39. Zimmerman, S. B., and Harrison, B. (1987) *Proc. Natl. Acad. Sci. U. S. A.* **84,** 1871–1875
40. Zimmerman, S. B., and Trach, S. O. (1988) *Biochim. Biophys. Acta* **949,** 297–304
41. Steensma, E., Heering, H. A., Hagen, W. R., and Van Mierlo, C. P. (1996) *Eur. J. Biochem.* **235,** 167–172
42. Hink, M. A., Borst, J. W., and Visser, A. J. (2003) *Methods Enzymol.* **361,** 93–112
43. Skakun, V. V., Hink, M. A., Digris, A. V., Engel, R., Novikov, E. G., Apanasovich, V. V., and Visser, A. J. (2005) *Eur. Biophys. J.* **34,** 323–334
44. Hess, S. T., Huang, S., Heikal, A. A., and Webb, W. W. (2002) *Biochemistry* **41,** 697–705
45. Chattopadhyay, K., Saffarian, S., Elson, E. L., and Frieden, C. (2005) *Biophys. J.* **88,** 1413–1422
46. Lakowicz, J. R. (1999) *Principles of Fluorescence Spectroscopy*, 2nd ed., Kluwer Academic/Plenum Publishers, New York
47. Babul, J., and Stellwagen, E. (1969) *Anal. Biochem.* **28,** 216–221
48. Knox, R. S., and van Amerongen, H. (2002) *J. Phys. Chem. B* **106,** 5289–5293
49. Toptygin, D., Savtchenko, R. S., Meadow, N. D., Roseman, S., and Brand, L. (2002) *J. Phys. Chem. B* **106,** 3724–3734
50. Nienhaus, G. U. (2006) *Macromol. Biosci.* **6,** 907–922
51. del Pino, I. M. P., Ibarra-Molero, B., and Sanchez-Ruiz, J. M. (2000) *Proteins* **40,** 58–70
52. Duy, C., and Fitter, J. (2006) *Biophys. J.* **90,** 3704–3711
53. Gellerich, F. N., Laterveer, F. D., Korzeniewski, B., Zierz, S., and Nicolay, K. (1998) *Eur. J. Biochem.* **254,** 172–180
54. Duy, C., and Fitter, J. (2005) *J. Biol. Chem.* **280,** 37360–37365
55. Stagg, L., Zhang, S. Q., Cheung, M. S., and Wittung-Stafshede, P. (2007) *Proc. Natl. Acad. Sci. U. S. A.* **104,** 18976–18981
56. Langdon, G. M., Jimenez, M. A., Genzor, C. G., Maldonado, S., Sancho, J., and Rico, M. (2001) *Proteins* **43,** 476–488

57. Muralidhara, B. K., and Wittung-Stafshede, P. (2004) *Biochemistry* **43,** 12855–12864
58. Wilkins, D. K., Grimshaw, S. B., Receveur, V., Dobson, C. M., Jones, J. A., and Smith, L. J. (1999) *Biochemistry* **38,** 16424–16431
59. Rajan, R. S., Illing, M. E., Bence, N. F., and Kopito, R. R. (2001) *Proc. Natl. Acad. Sci. U. S. A.* **98,** 13060–13065
60. Speed, M. A., Wang, D. I. C., and King, J. (1996) *Nat. Biotechnol.* **14,** 1283–1287
61. London, J., Skrzynia, C., and Goldberg, M. E. (1974) *Eur. J. Biochem.* **47,** 409–415
62. Betts, S., Haase-Pettingell, C., and King, J. (1997) *Adv. Protein Chem.* **50,** 243–264
63. Jaenicke, R., and Seckler, R. (1997) *Adv. Protein Chem.* **50,** 1–59
64. Ellis, R. J., and Hartl, F. U. (1999) *Curr. Opin. Struct. Biol.* **9,** 102–110
65. Frydman, J. (2001) *Annu. Rev. Biochem.* **70,** 603–647
66. van den Berg, B., Wain, R., Dobson, C. M., and Ellis, R. J. (2000) *EMBO J.* **19,** 3870–3875
67. Cheung, M. S., Klimov, D., and Thirumalai, D. (2005) *Proc. Natl. Acad. Sci. U. S. A.* **102,** 4753–4758
68. Hartl, F. U., and Hayer-Hartl, M. (2002) *Science* **295,** 1852–1858
69. Kaiser, C. M., Chang, H.-C., Agashe, V. R., Lakshmipathy, S. K., Etchells, S. A., Hayer-Hartl, M., Hartl, F. U., and Barral, J. M. (2006) *Nature* **444,** 455–460
70. Rüdiger, S., Germeroth, L., Schneider-Mergener, J., and Bukau, B. (1997) *EMBO J.* **16,** 1501–1507
71. Kerner, M. J., Naylor, D. J., Ishihama, Y., Maier, T., Chang, H. C., Stines, A. P., Georgopoulos, C., Frishman, D., Hayer-Hartl, M., Mann, M., and Hartl, F. U. (2005) *Cell* **122,** 209–220
72. Ogston, A. G. (1958) *Trans. Faraday Soc.* **54,** 1754–1757
73. Laurent, T. C., and Killander, J. (1964) *J. Chromatogr.* **14,** 317–330
74. Hoffmann, A., Kane, A., Nettels, D., Hertzog, D. E., Baumgartel, P., Lengefeld, J., Reichardt, G., Horsley, D. A., Seckler, R., Bakajin, O., and Schuler, B. (2007) *Proc. Natl. Acad. Sci. U. S. A.* **104,** 105–110